

phys. stat. sol. (b) **54**, 469 (1972)

Subject classification: 13.5; 6; 13.1; 14; 18.1; 20.1

*Zentralinstitut für Festkörperphysik und Werkstofforschung  
der Akademie der Wissenschaften der DDR, Dresden (a),  
and Sektion Physik der Technischen Universität Dresden,  
Arbeitsgruppe Theoretische Physik, Dresden (b)*

## On the Numerical Calculation of the Density of States and Related Properties

By

G. LEHMANN (a) and M. TAUT (b)

A method is given for the numerical calculation of energy surface integrals within the Brillouin zone like density of states, conductivity, susceptibility, dielectric function etc. The Brillouin zone is divided into tetrahedrons in which the integrand is interpolated linearly. In this way the integration can be done analytically avoiding the histogram method. Several similar methods are discussed with regard to the quotient of accuracy and effort.

Es wird eine Methode zur numerischen Berechnung von Integralen über Energieflächen in der Brillouin-Zone wie Zustandsdichte, Leitfähigkeit, Suszeptibilität, dielektrische Funktion u. a. angegeben. Die Brillouin-Zone wird in Tetraeder eingeteilt, in denen der Integrand linear interpoliert wird. Dadurch kann die Integration unter Vermeidung der Histogramm-Methode analytisch durchgeführt werden. Mehrere ähnliche Methoden werden hinsichtlich des Verhältnisses von Genauigkeit und Aufwand diskutiert.

### 1. Introduction

Calculating the density of states  $D(\varepsilon)$  of elementary excitations and other related integrals over the Brillouin zone listed in Section 2 often histogram methods have been used. They imply in principle serious complications as the statistical noise of the calculated function. The mean relative fluctuation of  $D(\varepsilon)$  in an energy interval is inversely proportional to the square root of the number of points in that interval. Decreasing the width of intervals results in an increase of statistical noise. If fine peaks in  $D(\varepsilon)$  shall be described a very large number of points must be calculated in order to distinguish between virtual statistical peaks and real ones. This situation was the reason for developing other calculation schemes for the density of states and related quantities [1, 2, 3, 5]. Gilat and Raubenheimer [1] (GR) divided the  $\mathbf{k}$ -space into cubes with equal volume and described the phonon dispersion relation within the cubes by a linear interpolation expression for which the density of states can be evaluated analytically. Lipton and Jacobs [2] (LJ) used a similar method as GR for the calculation of the spin susceptibility of metals. Whereas GR use for the interpolation the values of  $\varepsilon(\mathbf{k})$  and  $\text{grad } \varepsilon(\mathbf{k})$  at the centres of the cubes LJ employ the values of  $\varepsilon(\mathbf{k})$  at the corners of the cubes what reduces the numerical effort. The similar treatment of Lehmann et al. [3] starts from the fact that the coefficients of the linear interpolation expression in a tetrahedron are determined uniquely by the values of  $\varepsilon(\mathbf{k})$  at the corners of the tetrahedron. In this way a continuous interpolation over the total Brillouin zone is got and there are no

boundary effects. Moreover, the resulting formulas are very handy. The use of higher than linear interpolation expressions for  $\varepsilon(\mathbf{k})$ , like in the QUAD method (e.g. [4]), makes the analytical determination of  $D(\varepsilon)$  impossible. Therefore, Cooke and Wood [5] proposed a treatment which combines the QUAD and the GR method.

As recently the interest in that problem increased our treatment is reformulated in more detail in Section 3. A comparison of the mentioned three different linear schemes for the numerical calculation of the density of states is given and the relation of accuracy to numerical effort is discussed in Section 4. In Section 5 the results of some numerical tests are given.

## 2. Applications of the Method

In this Section some examples for physical quantities for the calculation of which our method is applicable are given. In Section 3 we shall describe the evaluation of integrals of type

$$\int \frac{dS}{|\text{grad } \Delta\varepsilon(\mathbf{k})|} A(\mathbf{k}) \quad (2.1)$$

over surfaces  $\Delta\varepsilon(\mathbf{k}) = \text{const}$  and in the Appendix integrals of type

$$\int \frac{dS}{|\text{grad } \Delta\varepsilon(\mathbf{k})|} A(\mathbf{k}) \theta(\varepsilon(\mathbf{k}) - \varepsilon_F) \quad (2.2)$$

over surfaces  $\Delta\varepsilon(\mathbf{k}) = \text{const}$  are reduced to (2.1).  $\theta(x)$  is the usual step function which coincides with the Fermi distribution function at temperature  $T = 0$ .

(i) At first the density of states of elementary excitations with the dispersion relation  $\varepsilon(\mathbf{k})$  is mentioned. The equation

$$D(\varepsilon) \propto \int_{\varepsilon(\mathbf{k}) = \varepsilon} \frac{dS}{|\text{grad } \varepsilon(\mathbf{k})|} \quad (2.3)$$

has the form (2.1).

(ii) The inverse of the effective mass tensor averaged over the occupied states can be transformed into an Fermi surface integral of the form (2.1):

$$\overline{m^{*-1}} \propto \int_{\varepsilon(\mathbf{k}) = \varepsilon_F} \frac{dS}{|\text{grad } \varepsilon(\mathbf{k})|} \text{grad } \varepsilon(\mathbf{k}) \circ \text{grad } \varepsilon(\mathbf{k}), \quad (2.4)$$

where  $\circ$  means the tensor product.

(iii) The conductivity in the direction  $\mathbf{e}$  due to crystal imperfections with the potential  $W$  can be calculated by means of a Fermi surface integral:

$$\mathbf{e} \sigma \mathbf{e} \propto \int_{\varepsilon(\mathbf{k}) = \varepsilon_F} \frac{dS}{|\text{grad } \varepsilon(\mathbf{k})|} \tau_{\mathbf{k}} (\mathbf{e} \text{grad } \varepsilon(\mathbf{k}))^2. \quad (2.5)$$

The relaxation time  $\tau_{\mathbf{k}}$  is in the Born approximation a Fermi surface integral equation which can be solved iteratively [6].

$$\tau_{\mathbf{k}}^{-1} \propto \int_{\varepsilon(\mathbf{k}) = \varepsilon_F} \frac{dS'}{|\text{grad } \varepsilon(\mathbf{k}')|} |\langle \psi_{\mathbf{k}} | W | \psi_{\mathbf{k}'} \rangle|^2 \left( 1 - \frac{\tau_{\mathbf{k}'} \mathbf{e} \text{grad } \varepsilon(\mathbf{k}')}{\tau_{\mathbf{k}} \mathbf{e} \text{grad } \varepsilon(\mathbf{k})} \right). \quad (2.6)$$

(iv) The real part of the magnetic susceptibility can be transformed into surface integrals of type (2.2) [2]:

$$\text{Re } \chi_0(\mathbf{q}, \omega) \propto P \sum_{\mu, \nu} \int d\Delta \frac{1}{\Delta - \hbar \omega} \int_{\Delta^{\mu\nu}(\mathbf{k}, \mathbf{q}) = \Delta} \frac{dS}{|\text{grad } \Delta^{\mu\nu}(\mathbf{k}, \mathbf{q})|} [f(\mathbf{k} + \mathbf{q}, \mu) - f(\mathbf{k}, \nu)]. \tag{2.7}$$

(v) The imaginary part of the macroscopic dielectric function in semiconductors often is calculated by means of [7]:

$$\text{Im } \epsilon(\omega) \propto \sum_i^{\text{occ.}} \sum_j^{\text{unocc.}} \int_{\omega^i(\mathbf{k}) = \omega} \frac{dS}{|\text{grad } \omega^{ij}(\mathbf{k})|} |M^{ij}(\mathbf{k})|^2. \tag{2.8}$$

### 3. Method

For the evaluation of integrals  $\mathcal{J}(\epsilon)$  over the surface  $\Delta\epsilon(\mathbf{k}) = \epsilon$ ,

$$\mathcal{J}(\epsilon) = \int \frac{dS}{|\text{grad } \Delta\epsilon(\mathbf{k})|} A(\mathbf{k}), \tag{3.1}$$

the Brillouin zone is divided into tetrahedrons with arbitrary shape but the same volume (it is not a necessary condition but simplifies the evaluation). Within the tetrahedrons  $\Delta\epsilon(\mathbf{k})$  is interpolated by a linear function:

$$\Delta\epsilon(\mathbf{k}) = \Delta\epsilon_0 + \mathbf{b} \mathbf{k}. \tag{3.2}$$

The coefficients  $\Delta\epsilon_0$  and  $\mathbf{b}$  are determined using the values of  $\Delta\epsilon(\mathbf{k}_i) = \Delta\epsilon_i$  at the corners  $\mathbf{k}_0 = 0$  and  $\mathbf{k}_i$  ( $i = 1, 2, 3$ ) of the tetrahedron (see Fig. 1). Using the triple  $\mathbf{r}_i$  contragredient to  $\mathbf{k}_i$

$$\mathbf{r}_j \mathbf{k}_i = \delta_{ij}; \quad \mathbf{r}_1 = \frac{\mathbf{k}_2 \times \mathbf{k}_3}{v}; \quad \mathbf{r}_2 = \frac{\mathbf{k}_3 \times \mathbf{k}_1}{v}; \quad \mathbf{r}_3 = \frac{\mathbf{k}_1 \times \mathbf{k}_2}{v}. \tag{3.3}$$

$\mathbf{b}$  is expressed as

$$\mathbf{b} = \sum_{i=1}^3 (\Delta\epsilon_i - \Delta\epsilon_0) \mathbf{r}_i. \tag{3.4}$$

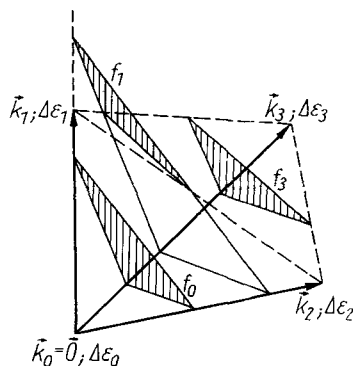


Fig. 1. One tetrahedron spanned out by the vectors  $0, \mathbf{k}_1, \mathbf{k}_2,$  and  $\mathbf{k}_3$ . The hatched planes are planes of constant  $\Delta\epsilon$ . Further explanation see in the text

$v = [\mathbf{k}_1, \mathbf{k}_2, \mathbf{k}_3]$  is the volume of the tetrahedron times six. The interpolated function  $\Delta\varepsilon(\mathbf{k})$  in the total Brillouin zone is continuous also at the boundaries of the tetrahedrons (it was not so in the papers of GR and LJ). Furthermore, it is not necessary to treat regions at the boundary of the Brillouin zone separately since the Brillouin zone may be divided into tetrahedrons totally.

In most cases the function  $A(\mathbf{k})$  can be interpolated linearly [8] within each tetrahedron like  $\Delta\varepsilon(\mathbf{k})$  in (3.2). (The case if  $A(\mathbf{k})$  contains the discontinuous step function is treated in the Appendix.)

$$a(\mathbf{k}) = a_0 + \mathbf{a} \mathbf{k} \quad (3.5)$$

Then  $\mathbf{a}$  is determined in analogy to (3.4). However, if  $A(\mathbf{k})$  depends on  $\mathbf{k}$  via  $\text{grad } \Delta\varepsilon(\mathbf{k})$  we take  $\text{grad } \Delta\varepsilon(\mathbf{k}) = \mathbf{b}$  with  $\mathbf{b}$  from (3.4) and insert this into  $A(\text{grad } \Delta\varepsilon(\mathbf{k}))$ .

With (3.5) the integral (3.1) over one tetrahedron consists of two parts:

$$i(\varepsilon) = a_0 i_0(\varepsilon) + \mathbf{a} \mathbf{i}_1(\varepsilon) \quad (3.6)$$

where

$$i_0(\varepsilon) = \int_{\Delta\varepsilon(\mathbf{k})=\varepsilon} \frac{dS}{|\mathbf{b}|} \quad (3.7)$$

and

$$\mathbf{i}_1(\varepsilon) = \int_{\Delta\varepsilon(\mathbf{k})=\varepsilon} \frac{dS}{|\mathbf{b}|} \mathbf{k} \quad (3.8)$$

$i_0(\varepsilon)$  is the density of states from one tetrahedron which can be written as

$$i_0(\varepsilon) = f(\varepsilon) \cdot |\mathbf{b}|^{-1},$$

where  $f(\varepsilon)$  is the cross section of the plane  $\Delta\varepsilon(\mathbf{k}) = \varepsilon$  with the tetrahedron.  $f(\varepsilon)$  may be written as a sum of triangular areas determined by the intersections of the plane  $\Delta\varepsilon(\mathbf{k}) = \varepsilon$  with the space corner put up by the following straight lines in Fig. 1.

$$\overline{01}, \overline{02}, \overline{03} \quad (f_0); \quad \overline{10}, \overline{12}, \overline{13} \quad (f_1); \quad \overline{30}, \overline{31}, \overline{32} \quad (f_3).$$

With ordered energies according to  $\Delta\varepsilon_0 < \Delta\varepsilon_1 < \Delta\varepsilon_2 < \Delta\varepsilon_3$  we get

$$f(\varepsilon) = \begin{cases} f_0 & \Delta\varepsilon_0 \leq \varepsilon \leq \Delta\varepsilon_1 \\ f_0 - f_1 & \text{for } \Delta\varepsilon_1 \leq \varepsilon \leq \Delta\varepsilon_2 \\ f_3 & \Delta\varepsilon_2 \leq \varepsilon \leq \Delta\varepsilon_3, \end{cases} \quad (3.9)$$

where

$$\left. \begin{aligned} f_0 |\mathbf{b}|^{-1} &= \frac{v}{2} \frac{(\varepsilon - \Delta\varepsilon_0)^2}{(\Delta\varepsilon_1 - \Delta\varepsilon_0)(\Delta\varepsilon_2 - \Delta\varepsilon_0)(\Delta\varepsilon_3 - \Delta\varepsilon_0)} \\ f_1 |\mathbf{b}|^{-1} &= \frac{v}{2} \frac{(\varepsilon - \Delta\varepsilon_1)^2}{(\Delta\varepsilon_1 - \Delta\varepsilon_0)(\Delta\varepsilon_2 - \Delta\varepsilon_1)(\Delta\varepsilon_3 - \Delta\varepsilon_1)} \\ f_3 |\mathbf{b}|^{-1} &= \frac{v}{2} \frac{(\varepsilon - \Delta\varepsilon_3)^2}{(\Delta\varepsilon_3 - \Delta\varepsilon_0)(\Delta\varepsilon_3 - \Delta\varepsilon_1)(\Delta\varepsilon_3 - \Delta\varepsilon_2)}. \end{aligned} \right\} \quad (3.10)$$

<sup>1)</sup> Quantities resulting from one tetrahedron are denoted by small letters.

As a remarkable result  $i_0(\varepsilon)$  depends only on the energy values  $\Delta\varepsilon_0, \Delta\varepsilon_1, \Delta\varepsilon_2, \Delta\varepsilon_3$  and the volume of the tetrahedron but not on the shape of the tetrahedron. Furthermore  $i_0(\varepsilon)$  is a quadratic polynomial in  $\varepsilon$ . Therefore, the function  $i_0(\varepsilon)$  may be characterized by its constant second derivative  $i_0''$  in each energy interval. Then  $i_0'(\varepsilon)$  and  $i_0(\varepsilon)$  may be calculated from  $i_0''$  by means of the conditions that  $i_0(\varepsilon)$  and  $i_0'(\varepsilon)$  are continuous at the points  $\Delta\varepsilon_i$ .

For the calculation of the contribution  $\mathcal{J}_0(\varepsilon)$  coming from the first term in (3.6) by summation over all tetrahedrons of one band we take the following procedure. Firstly all energy values  $E_L$  of one band are ordered:  $E_L \leq E_{L+1}$ . The energy interval between  $E_L$  and  $E_{L+1}$  is characterized by the number  $L$ . The aim is to express  $\mathcal{J}_0(\varepsilon)$  in each interval as an analytical (parabola) function. Now for each tetrahedron the second derivative is calculated for the three regions between  $\Delta\varepsilon_0$  and  $\Delta\varepsilon_1$ ,  $\Delta\varepsilon_1$  and  $\Delta\varepsilon_2$ , and  $\Delta\varepsilon_2$  and  $\Delta\varepsilon_3$ . In each region  $i_0''$  is a constant. Then those second derivatives multiplied by the appropriate  $\alpha_0$  are stored in the intervals lying between  $\Delta\varepsilon_0$  and  $\Delta\varepsilon_1$ ,  $\Delta\varepsilon_1$  and  $\Delta\varepsilon_2$ , and  $\Delta\varepsilon_2$  and  $\Delta\varepsilon_3$ . The contributions of all tetrahedrons are summed up. Thus the second derivative coming from all tetrahedrons of the Brillouin zone is obtained.  $\mathcal{J}_0''(\varepsilon)$  is constant in each energy interval.  $\mathcal{J}_0'(\varepsilon)$  and  $\mathcal{J}_0(\varepsilon)$  we get by integration taking into account the continuity and the smoothness at the boundaries  $E_L$  of the energy intervals.

The evaluation of  $i_1(\varepsilon)$  gives in a similar way as for  $i_0(\varepsilon)$

$$i_1(\varepsilon) = f(\varepsilon) |\mathbf{b}|^{-1} \mathbf{s}(\varepsilon), \quad (3.11)$$

where  $\mathbf{s}(\varepsilon)$  is the centre of gravity of  $f(\varepsilon)$ .

$$\mathbf{s}(\varepsilon) = \begin{cases} \mathbf{s}_0 & \Delta\varepsilon_0 \leq \varepsilon \leq \Delta\varepsilon_1 \\ \frac{\mathbf{s}_0 f_0 - \mathbf{s}_1 f_1}{f_0 - f_1} & \text{for } \Delta\varepsilon_1 \leq \varepsilon \leq \Delta\varepsilon_2 \\ \mathbf{s}_3 & \Delta\varepsilon_2 \leq \varepsilon \leq \Delta\varepsilon_3. \end{cases} \quad (3.12)$$

The  $\mathbf{s}_i$  are the centres of gravity of the appropriate triangles  $f_i$ .

$$\mathbf{s}_i(\varepsilon) = \mathbf{k}_i + \frac{(\varepsilon - \Delta\varepsilon_i)}{3} \sum_{\substack{j=0 \\ (j \neq i)}}^3 \frac{(\mathbf{k}_j - \mathbf{k}_i)}{(\Delta\varepsilon_j - \Delta\varepsilon_i)}. \quad (3.13)$$

In (3.12) the case  $\Delta\varepsilon_1 \leq \varepsilon \leq \Delta\varepsilon_2$  has an involved structure. Therefore, it may be more appropriate to approximate it by the following linear expression:

$$\bar{\mathbf{s}}(\Delta\varepsilon_1 \leq \varepsilon \leq \Delta\varepsilon_2) \approx \frac{(\varepsilon - \Delta\varepsilon_2)}{(\Delta\varepsilon_1 - \Delta\varepsilon_2)} \mathbf{s}_0(\Delta\varepsilon_1) + \frac{(\varepsilon - \Delta\varepsilon_1)}{(\Delta\varepsilon_2 - \Delta\varepsilon_1)} \mathbf{s}_3(\Delta\varepsilon_2). \quad (3.14)$$

Unfortunately,  $i_1$  and  $\mathbf{s}$  are dependent on the geometry of the tetrahedrons and cannot be characterized in such a simple way as  $i_0$  by its derivatives.

#### 4. Comparison of the Accuracy of Our Method with Other Ones

In this section the accuracy of different approaches is checked by investigating the mean squared deviations  $\overline{\delta f^2}$  of different linear interpolation expressions  $f_{A,B,C,D}$  from a complete quadratic function  $f$ ,

$$f = a_1 x^2 + a_2 y^2 + a_3 z^2 + a_4 yz + a_5 xz + a_6 xy + a_7 + a_8 x + a_9 y + a_{10} z. \quad (4.1)$$

The deviations  $\overline{\delta f^2}$  from (4.1) are representative for nonsingular smooth functions and small cells (linear dimension  $2\alpha$ ). They are proportional to  $\alpha^4$ . Third order terms in (4.1) give higher order corrections in  $\alpha$ . The different interpolation expressions are:

$$f_A = a_7 + a_8 x + a_9 y + a_{10} z \quad (\text{Gilat/Raubenheimer}), \quad (4.2)$$

$$f_B = (a_1 + a_2 + a_3)\alpha^2 + a_7 + a_8 x + a_9 y + a_{10} z \quad (\text{Lipton/Jacobs}), \quad (4.3)$$

where  $f_A$  and  $f_B$  hold within a cube of edge length  $2\alpha$ .

$f_C$ : our expressions, where the same cube as in A and B is divided in six tetrahedrons with corners at the following points: (111), (11 $\bar{1}$ ), (1 $\bar{1}$ 1), ( $\bar{1}$ 11); (1 $\bar{1}$ 1), ( $\bar{1}$ 11), ( $\bar{1}\bar{1}$ 1); (111), ( $\bar{1}$ 11), (11 $\bar{1}$ ), ( $\bar{1}$ 11); (111), (1 $\bar{1}$ 1), (111), ( $\bar{1}$ 11); (11 $\bar{1}$ ), ( $\bar{1}$ 11), ( $\bar{1}\bar{1}$ 1); (111), (1 $\bar{1}$ 1), (11 $\bar{1}$ ), ( $\bar{1}\bar{1}$ 1).

$f_D$ : our expression, where the mesh in the  $xy$ -plane consists of equilateral triangles (length  $2\alpha$ ), the different layers have in  $z$ -direction the distance  $2\alpha\zeta$  ( $\zeta$  arbitrary parameter), every prism is then divided into three tetrahedrons with corners at the points:  $(1, -\sqrt{3}/3, \zeta)$ ,  $(-1, -\sqrt{3}/3, \zeta)$ ,  $(0, 2\sqrt{3}/3, \zeta)$ ,  $(0, 2\sqrt{3}/3, -\zeta)$ ;  $(1, -\sqrt{3}/3, \zeta)$ ,  $(-1, -\sqrt{3}/3, \zeta)$ ,  $(-1, -\sqrt{3}/3, -\zeta)$ ,  $(0, 2\sqrt{3}/3, -\zeta)$ ;  $(1, -\sqrt{3}/3, -\zeta)$ ,  $(-1, -\sqrt{3}/3, -\zeta)$ ,  $(0, 2\sqrt{3}/3, -\zeta)$ ,  $(1, -\sqrt{3}/3, \zeta)$ . The coefficients of the reduced (on the same density of mesh points) mean squared deviation  $\overline{\delta f_{\text{red}}^2}$ ,

$$\overline{\delta f_{\text{red}}^2} = \Omega^{-4/3} \overline{\delta f^2} = \sum_{i,j=1}^6 c_{ij} a_i a_j, \quad (4.4)$$

are presented in Table 1.  $\Omega$  is the volume of the primitive cell of the mesh (A, B, and C:  $\Omega = 8\alpha^3$ ; D:  $\Omega = 4\sqrt{3}\alpha^3\zeta$ ). The coefficients  $c_{ij}$  of the mixed terms in (4.4) except  $c_{12}$  are emitted in Table 1 because they can give to  $\overline{\delta f_{\text{red}}^2}$  both positive or negative contributions. The  $c_{ii}$  for  $i > 6$  vanish. It can be seen from the Table that approach A is better than B, C, D by a factor 1 to 3. The differences between B, C, and D are smaller. The best of the last three is approach D. However, in method A one has to calculate at every mesh point four quantities ( $f$  and  $\text{grad } f$ ), whereas for methods B, C, and D only  $f$  must be calculated.

Table 1

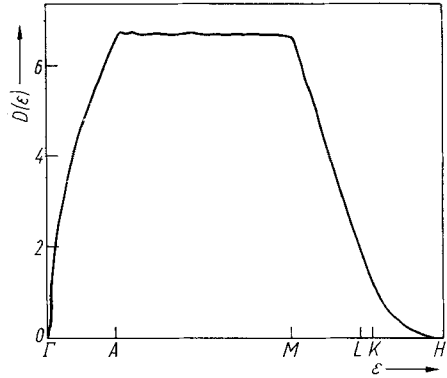
Coefficients  $c_{ij}$  of the reduced mean squared deviations defined in (4.4) for different interpolation expressions. From the non-diagonal coefficients only  $c_{12}$  is given

case	$c_{11} = c_{22}$	$c_{33}$	$c_{44}$	$c_{55}$	$c_{66}$	$c_{12}$
A	1/80	1/80	1/144	1/144	1/144	1/144
B	1/30	1/30	1/144	1/144	1/144	1/36
C	1/30	1/30	1/90	1/90	1/90	1/36
D	$\frac{1}{40} \sqrt[3]{\frac{3}{4}} \zeta^{-4/3}$	$\frac{2}{45} \sqrt[3]{\frac{3}{4}} \zeta^{8/3}$	$\frac{1}{90} \sqrt[3]{\frac{3}{4}} \zeta^{2/3}$	$\frac{1}{135} \sqrt[3]{\frac{3}{4}} \zeta^{2/3}$	$\frac{1}{360} \sqrt[3]{\frac{3}{4}} \zeta^{-4/3}$	$\frac{7}{360} \sqrt[3]{\frac{3}{4}} \zeta^{-4/3}$

### 5. Numerical Results

To test the accuracy of our method we calculated the density of states and its first and second derivative for the first free electron band in a hexagonal Brillouin zone. The results are given in Fig. 2 to 4 for a mesh of 222 points in 1/24 Brillouin

Fig. 2. Density of states  $D(\epsilon)$  of the first free electron band in a hexagonal Brillouin zone from 222 points in  $1/24$  zone using the present method



zone. The density of states  $D(\epsilon)$  in Fig. 2 shows so few deviations from the exact curve that it is redundant to include the latter in Fig. 2. The first derivative  $D'(\epsilon)$  calculated by our method and the exact curve are given in Fig. 3. We see that the deviation is marked but not too large. In the second derivative  $D''(\epsilon)$  given in Fig. 4, however, the statistical noise is too large to use our method. An calculation with 819 points in  $1/24$  Brillouin zone gave no satisfactory progress in decreasing the statistical fluctuations.

Moreover the area of constant energy surfaces and the mean electron velocity averaged over a constant energy surface are calculated and given in Fig. 5 and 6, respectively. Again 222 points in  $1/24$  Brillouin zone and a free electron band are used. The energy surface  $F(\epsilon)$  calculated with our method agrees so good with the exact curve that the latter is not included in Fig. 5.

The results show that a number of points of order 200 is enough to give numerical surface integrals with an accuracy of about 1%. For the energy derivatives of such quantities much more points are necessary.

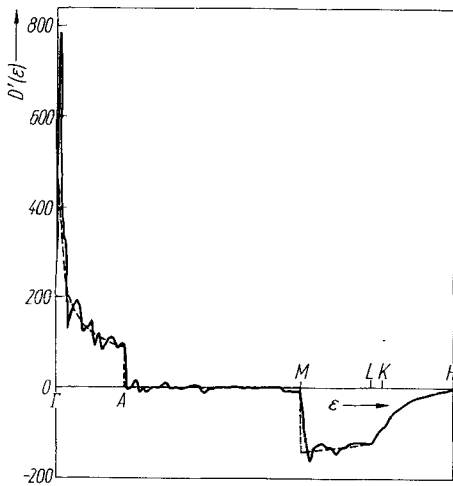


Fig. 3. First derivative  $dD(\epsilon)/d\epsilon$  of Fig. 2 (full line). The dashed line is the exact result for  $dD(\epsilon)/d\epsilon$

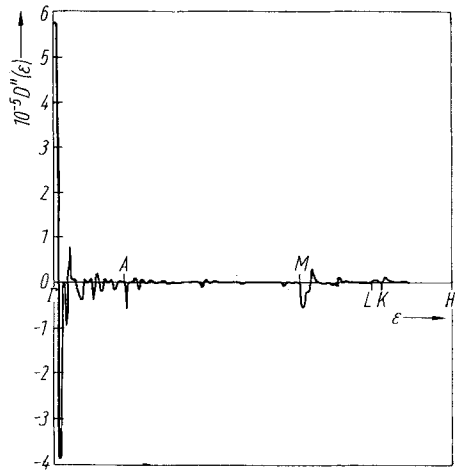


Fig. 4. Second derivative  $d^2D(\epsilon)/d\epsilon^2$  of Fig. 2

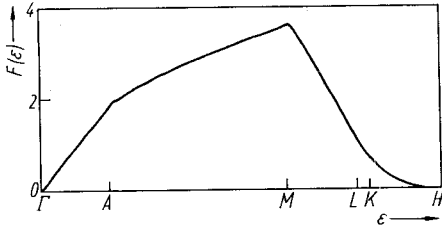


Fig. 5. The area  $F(\epsilon)$  of the constant energy surfaces of the first free electron band in a hexagonal Brillouin zone from 222 points in  $1/24$  zone

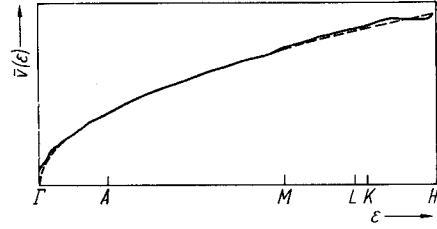


Fig. 6. The mean velocity  $v$  averaged over constant energy surfaces of the first free electron band in a hexagonal Brillouin zone from 222 points on  $1/24$  zone (full line). The dashed line is the exact result

**Acknowledgement**

The authors are indebted to the members of the group “Elektronenstruktur” at the Section Physik, TU Dresden, for critical discussions.

**Appendix**

In this Appendix we describe how integrals of type (2.2),

$$\int_{\Delta\epsilon(\mathbf{k})=\epsilon} \frac{dS}{|\text{grad } \Delta\epsilon(\mathbf{k})|} A(\mathbf{k}) \theta(\epsilon(\mathbf{k}) - \epsilon_F). \tag{A.1}$$

are treated in the framework of our tetrahedron method. We assume  $\Delta\epsilon(\mathbf{k})$  and  $\epsilon(\mathbf{k})$  to be given at a mesh of points in the Brillouin zone. Again the Brillouin zone is divided into tetrahedrons and only one tetrahedron is considered. Also  $\epsilon(\mathbf{k})$  is interpolated linearly in one tetrahedron according to (3.2) and (3.4),

$$\epsilon(\mathbf{k}) = \epsilon_0 + \mathbf{c} \mathbf{k}. \tag{A.2}$$

The step function  $\theta(\epsilon(\mathbf{k}) - \epsilon_F)$  restricts the integration to a part of the tetrahedron. The boundary planes  $\epsilon(\mathbf{k}) = \epsilon_F$  are shown in Fig. 7 in the following three cases:

I. 
$$\epsilon_0 \leq \epsilon_F \leq \epsilon_1.$$

The integral (A.1) is restricted to the small tetrahedron characterized by the corners  $0, \mathbf{k}_{01}^I, \mathbf{k}_{02}^I,$  and  $\mathbf{k}_{03}^I$ . The  $\mathbf{k}_{0i}^I$  and the  $\Delta\epsilon_{0i}^I$  can be calculated by the following equations:

$$\begin{aligned} \mathbf{k}_{0i}^I &= \frac{(\epsilon_F - \epsilon_0)}{(\epsilon_i - \epsilon_0)} \mathbf{k}_i = \frac{(\epsilon_F - \epsilon_0)}{\mathbf{c} \mathbf{k}_i} \mathbf{k}_i, \\ \Delta\epsilon_{0i}^I &= \Delta\epsilon_0 + \mathbf{b} \mathbf{k}_{0i}^I. \end{aligned} \tag{A.3} \quad (i = 1, 2, 3)$$

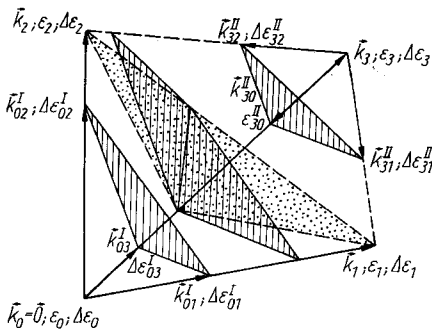


Fig. 7. The reduction of integrals of type (2.2) to integrals of type (2.1). The hatched regions are planes  $\epsilon(\mathbf{k}) = \epsilon_F$ . Further explanation see in the text

This small tetrahedron is treated in the usual way described in Section 3.

II.

$$\varepsilon_2 \leq \varepsilon_F \leq \varepsilon_3 .$$

The integral covers almost the whole tetrahedron except the small one given by the corners  $\mathbf{k}_3$ ,  $\mathbf{k}_3 + \mathbf{k}_{30}^{\text{II}}$ ,  $\mathbf{k}_3 + \mathbf{k}_{31}^{\text{II}}$ , and  $\mathbf{k}_3 + \mathbf{k}_{32}^{\text{II}}$ . We account for the whole tetrahedron in the usual way and subtract the contribution of the little one with the following parameters:

$$\begin{aligned} \mathbf{k}_{3i}^{\text{II}} &= \frac{(\varepsilon_F - \varepsilon_3)}{c(\mathbf{k}_3 - \mathbf{k}_i)} (\mathbf{k}_3 - \mathbf{k}_i), \\ \Delta\varepsilon_{3i}^{\text{II}} &= \Delta\varepsilon_0 + b \mathbf{k}_{3i}^{\text{II}} . \end{aligned} \quad (i = 0, 1, 2) \quad (\text{A.4})$$

III.

$$\varepsilon_1 \leq \varepsilon_F \leq \varepsilon_2 .$$

The primary tetrahedron is divided in two secondary ones by the dotted plane in Fig. 7. Now we have one tetrahedron for case I and one for case II. The vectors of the additional corner and the appropriate energy can be calculated by (A.3) and (A.4).

We see that an important advantage of the tetrahedron method is the reduction of integrals of type (2.2) to those of type (2.1).

### References

- [1] G. GILAT and L. J. RAUBENHEIMER, Phys. Rev. **144**, 390 (1966).
- [2] D. LIPTON and R. L. JACOBS, J. Phys. C **3**, 1388 (1970).
- [3] G. LEHMANN, P. RENNERT, M. TAUT, and H. WONN, phys. stat. sol. **37**, K27 (1970).
- [4] F. M. MUELLER, J. W. GARLAND, M. H. COHEN, and K. H. BENNEMANN, Ann. Phys. (U.S.A.) **67**, 19 (1971).
- [5] J. F. COOKE and R. F. WOOD, Phys. Rev. **B5**, 1276 (1972).
- [6] YUH FUKAI, Phys. Rev. **186**, 697 (1969).
- [7] L. R. SARAVIA and D. BRUST, Phys. Rev. **171**, 916 (1968).
- [8] N. W. DALTON, J. Phys. C **3**, 1912 (1970).

(Received July 21, 1972)